Kinetics and Mechanisms of the Oxidation of Hydrazine by Aqueous Iodine†

Rong Ming Liu and Dale W. Margerum*

Department of Chemistry, Purdue University, West Lafayette, Indiana 47907

Received June 17, 1997

Kinetics for the reactions of I_2 with excess $N_2H_5^+/N_2H_4$ and I^- are measured by the loss of I_3^- over a wide range of acidity from pH 0.35 to 8.0 at 25.0 °C, $\mu = 0.50$ M. Pseudo-first-order rate constants increase by factors of more than 10^7 with increase of pH, hydrazine, and buffer concentrations. Below pH 1, I_2 reacts directly with $N_2H_5^+$ which has a relative reactivity that is 2.4×10^7 times smaller than N_2H_4 (the dominant reactant at pH ≥ 1). Kinetic evidence for $IN_2H_4^+$ as a steady-state species is found below pH 3. From pH 3.5 to 6.3, rate constants are measured by stopped-flow methods and at higher pH by pulsed−accelerated-flow methods. A multistep mechanism is proposed where I_2 reacts rapidly with N_2H_4 to form an $I_2N_2H_4$ adduct ($K_A = 2.0 \times 10^4$ M^{-1}) that is present in appreciable concentrations above pH 6. The adduct undergoes general base-assisted deprotonation accompanied by loss of I^- in the rate-determining step. Subsequent intermediates react rapidly with another I_2 to form N_2 as a final product. At high pH, hydrazine acts as a general base as well as the initial nucleophile. Rate constants for various bases (H_2O, CH_3COO^-, HPO_4^{2-}, N_2H_4, and OH^-) fit a Brønsted β value of 0.46. Values for the second-order rate constants (M^{-1} s^{-1}) for $I_2N_2H_4$ reactions with CH_3COO^-, HPO_4^{2-}, N_2H_4, and OH^- are 7.5×10^3, 2.0×10^5, 8.5×10^5, and 4.8×10^8, respectively.

Introduction

Iodine oxidation of hydrazine to give dinitrogen is rapid and complete. The overall stoichiometry in eq 1 has been shown[1]

$$2I_2 + N_2H_4 \rightarrow N_2 + 4I^- + 4H^+ \quad (1)$$

to be valid from pH 1 to 9, and the reaction is used in titrimetric methods for the determination of hydrazine.[2] Although some reaction kinetics have been reported,[3−11] there is disagreement in regard to the mechanisms and the rate constants.

In 1975, Hasty[5] reported an iodide ion dependence study for iodine reactions with hydrazine at pH ∼ 1.3. He suggested that $N_2H_5^+$ reacted with HOI and with I_2. The large uncertainties of his data were subsequently questioned by King et al.,[6] who showed that at low pH, the reactive species were N_2H_4 and I_2. They suggested the mechanism in eqs 2 and 3, where a steady-state species, $IN_2H_4^+$, forms and decays to products with $k_1 = 4.4 \times 10^7$ M^{-1} s^{-1} and $k_{-1}/k_2 = 12.0$ M^{-1}, based on a pK_a value of 8.5 for $N_2H_5^+$. (We show that this pK_a is 8.06 at 25.0 °C, $\mu = 0.50$ M.)

$$I_2 + N_2H_4 \underset{k_{-1}}{\overset{k_1}{\rightleftharpoons}} IN_2H_4^+ + I^- \quad (2)$$

$$IN_2H_4^+ \xrightarrow{k_2} \text{products} \quad (3)$$

In 1985, Sultan et al.[8] also suggested that N_2H_4 and I_2 were the reactive species, but they failed to study the iodide ion dependence and gave no values for the rate constants. In 1986, Radhakrishnamurti et al.[9] reported that at high acidity (up to 2.0 M $[H^+]$) N_2H_4 reacts both with I_2 and with HOI. They reported an unreasonably large rate constant of 7.9×10^{10} M^{-1} s^{-1} for HOI path, which is an order of magnitude greater than the diffusion-controlled rate constant of 7.0×10^9 M^{-1} s^{-1}.[12] They also reported a saturation effect with increased $[N_2H_4]_T$ concentrations (5.0−50.0 mM), where k_{obsd} values are no longer linearly proportional to $[N_2H_4]_T$. In 1988, Janovsky[10] extended the kinetic studies to higher pH (5.5−7.0) in phosphate buffer by using pulse radiolysis. He agreed with earlier workers that N_2H_4 and I_2 are reactive species. He observed phosphate buffer catalysis, which was attributed to the formation of a $N_2H_4 \cdot HPO_4^{2-}$ complex. (This is very unlikely since both N_2H_4 and HPO_4^{2-} are nucleophiles.) In 1990, Rao and Dalvi[11] reported that there was no effect of acetate buffer concentration on the reaction rates.

The above overview of the reactions of hydrazine with iodine indicates that, in spite of past work, the kinetics and mechanisms of iodine oxidation of hydrazine are not well understood. We now report the kinetics of the I_2/I_3^- reaction with $N_2H_4/N_2H_5^+$ over a much wider pH range (0−8.0) than previously used. We test the effect of buffer, iodide ion, and reactant concentrations and show a general mechanism that fits all the data. We find no saturation effect at high hydrazine concentrations and show large effects due to buffers in base-assisted reactions.

† Dedicated to Professor Ralph G. Wilkins in recognition of his 70th birthday.

(1) Cooper, J. N.; Ramette, R. W. *J. Chem. Educ.* **1969,** *46,* 872−873.
(2) *Encyclopedia of Industrial Chemical Analysis;* Wiley: New York, **1971**; Vol. 14, p 232.
(3) Lumme, P.; Lahermo, P.; Tummavuori, J. *Acta Chem. Scand.* **1965,** *19,* 2175−2188.
(4) Klopman, G.; Tsuda, K.; Louis, J. B. Davis, R. E. *Tetrahedron* **1970**, *26,* 4549−54.
(5) Hasty, R. A. *Z. Phys. Chem.* **1975,** *94,* 53−61.
(6) King, S. E.; Cooper, J. N.; Crawford, R. D. *Inorg. Chem.* **1978,** *17,* 3306−3307.
(7) Gopalan, R.; Karunakaran, J. *Indian J. Chem.* **1980,** *19A,* 162−163.
(8) Sultan, S. M.; Al-Zamil, I. Z.; Al-Hajjaji, A. M.; Al-Tamrah, S. A.; Rahman, A. M. *J. Chem. Soc. Pak.* **1985,** *7,* 93−99.
(9) Radhakrishnamurt, P. S.; Rath, N. K.; Panda, R. K. *J. Chem. Soc., Dalton Trans.* **1986,** 1189−1192.
(10) Janovsky, I. *J. Radioanal. Nucl. Chem., Lett.* **1988,** *128,* 433−441.
(11) Rao, T. S.; Dalvi, S. P. *Proc. Indian Nat. Sci. Acad.* **1990,** *56A,* 153−160.
(12) Caldin, E. F. *Fast Reactions in Solution*; Wiley: London, 1964; pp 10−12.

S0020-1669(97)00753-2 CCC: $15.00
Published on Web 04/30/1998

Experimental Section

Reagents. Distilled, deionized water was purged with argon and used to prepare all solutions. Ionic strength (μ) was adjusted to 0.50 M with recrystallized $NaClO_4$ unless otherwise indicated. Acidity was adjusted with standardized $HClO_4$ solutions. An Orion model SA 720 Research pH meter and a Corning combination electrode were used to measure pH values, which were corrected to p[H^+] values at 25.0 °C and μ = 0.50 M based on electrode calibration by titration of standardized $HClO_4$ and NaOH. All chemicals were reagent grade. The concentrations given for kinetic reactions are postmixing values.

Stock solutions of 0.10 M $[I_2]_T$ were prepared by dissolving crystalline I_2 in 0.48 M KI solutions. Stock solutions of 0.200 M NaI were prepared from the crystalline solid and purged with Ar to remove dissolved O_2. These solutions were stored in the dark. Solutions of N_2H_4·HCl (Aldrich) were standardized with a standard 0.0250 M KIO_3 solution,[13] which was prepared from a primary solid KIO_3 (Baker, dried at 130 °C for 2 h). Stock solutions of 2.0 M $[HOAc]_T$ were prepared from dilution of glacial acetic acid, and buffer solutions were prepared by the addition of 1.0 M NaOH. Stock solutions of 0.50 M NaH_2PO_4 were prepared from the crystalline salt, and buffer solutions were made by the addition of 1.0 M NaOH.

Kinetic Measurements. All reactions were followed by the loss of I_3^- absorbance at 353 nm (ϵ_{I_3} = 26 400 M^{-1} cm^{-1})[14] in the presence of excess I^- and excess total hydrazine unless otherwise noted. Excellent pseudo-first-order rates were observed in accord with eq 4, where $[I_2]_T = [I_3^-] + [I_2] + [I_2N_2H_4]$ and k_r is a function of the concentrations of $[N_2H_4]_T$, $[I^-]$, $[H^+]$, and buffer. Each reported k_r value measured by stopped-flow or pulsed−accelerated-flow (PAF) instruments is an average of four to eight trials. All reactions were run at 25.0 ± 0.1 °C.

$$\frac{-\mathrm{d}[I_2]_T}{\mathrm{d}t} = k_r[I_2]_T \tag{4}$$

Slower reactions at low pH (with half-lives of 2 min to 5 h) were measured with a Perkin-Elmer Lambda-9 UV/vis/NIR spectrophotometer interfaced to a Zenith 386/20 computer.

Reactions in $HOAc/OAc^-$ buffer and in $H_2PO_4^-/HPO_4^{2-}$ buffer with half-lives of 2.3 ms to 4.0 s were monitored by a Durrum stopped-flow spectrophotometer (model D-110 with an optical pathlength of 1.88 cm) interfaced to a Zenith 151 PC with a Metrabyte DASH-16 A/D interface card. All k_{obsd} values greater than 60 s^{-1} were corrected for mixing limitations[15] of this instrument by using $k_r = k_{obsd}/[1 - (k_{obsd}/k_{mix})]$, where k_{mix} = 5.08 × 10^3 s^{-1}.

Faster reactions (above pH 6.9) with $N_2H_5^+/N_2H_4$ as self-buffer were measured by pulsed−accelerated-flow methods.[16−20] Solutions for all PAF experiments were filtered and degassed.

PAF Method with Integrating Observation. The PAF−IO (model IV) spectrophotometer[19] and previous PAF instruments have used integrating observation during continuous decelerated flow mixing of short duration (a 0.4 s pulse). The light path is along the direction of flow. The measured rate constant depends on the initial absorbance of the reactants, A_o, the absorbance at a given instantaneous velocity, A_v, and the final absorbance, A_∞. Pseudo-first-order rate constants, k_r, can be determined by using eq 5, where M_{exptl} represents the degree of reaction, b is the reaction path length (0.01025 m), υ is the solution velocity (12 to 3 m/s), and k_m is a proportionality constant from the mixing rate constant ($k_{mix} = k_m\upsilon$). In the PAF integrating observation

$$M_{exptl} = \frac{A_v - A_\infty}{A_o - A_\infty} = \frac{1}{bk_m} + \frac{\upsilon}{bk_r} \tag{5}$$

technique, the reactants are observed from the point where they initially mix until they exit the observation tube. The method is capable of measuring fast reactions with half-lives in the range of 4 μs to 1 ms. However, this PAF method requires knowledge of A_o. An extremely fast reaction that decreases A_o prior to the reaction under study will give observed k_r values that are too large. This problem can be overcome by use of the PAF-PRO instrument[20] in which observation is made across the flow rather than by integrated observation along the direction of flow.

Pulsed−Accelerated-Flow with Position-Resolved Observation (PAF-PRO). A new pulsed−accelerated-flow spectrometer with position-resolved observation has been developed in this laboratory.[20] The instrument utilizes a wider range of flow velocities (20 to 2 m/s) than the PAF-IV instrument and observation is perpendicular to solution flow at multiple points in the observation tube. A masked charge-coupled device (CCD) with 1024 × 1024 resolution elements in an 8 × 8 binning mode enables observation at 128 discrete positions along the observation tube (1.945 cm in length). The progress of the reaction is monitored as a function of distance the solution travels down the observation tube at 126 different flow velocities in the range of 19.7−2.2 m/s. Data for a single kinetic run are collected in 0.5 s with the consumption of 11.0 mL of each reagent. Since observation is perpendicular to solution flow, the optical path length is determined by the width of the observation tube (0.212 cm). Reaction half-lives can be measured in the range of 0.07−3 ms.

For pseudo-first-order reactions, the absorbance (A_p) is measured at 128 positions along the observation cell, and these positions are converted to the appropriate time scale for each flow velocity. The apparent rate constant, k_{app}, is evaluated from plots of $\ln(A_p - A_\infty)$ vs time for each of 126 different flow velocities. On the basis of earlier studies,[16,17] the physical mixing rate constant is proportional to the flow velocity ($k_{mix} = k_m\upsilon$) and eq 6 relates the apparent rate constant to the chemical reaction rate constant (k_r) and the mixing rate constant. A weighted linear regression analysis is used to evaluate k_r and k_m.

$$\frac{1}{k_{app}} = \frac{1}{k_m}\left(\frac{1}{\upsilon}\right) + \frac{1}{k_r} \tag{6}$$

Results and Discussion

Reaction kinetics for the loss of $[I_2]_T$ in the presence of both excess $[N_2H_4]_T$ and $[I^-]$ are studied as a function of $[H^+]$, $[I^-]$, $[N_2H_4]_T$, and buffer concentrations. We found no evidence of the saturation effect reported by Radhakrishnamurti et al.,[9] who claimed that at high concentrations of hydrazine (up to 50.0 mM $[N_2H_4]_T$) the reaction rate approached a limiting value. Our data (Table 1) show that the k_r values are linearly proportional to $[N_2H_4]_T$ from 4 to 100 mM at p[H^+] = 0.040 and increase greatly with increase of $[N_2H_4]_T$ at p[H^+] = 7.2. We agree with previous work that suggested N_2H_4 is far more reactive than $N_2H_5^+$ and that I_2 is reactive while I_3^- is not. In general, the k_r values decrease with I^- concentration due to the formation of I_3^-. At low pH additional I^- inhibition occurs due to the reverse reaction in eq 2. Figure 1 shows that the values of the pseudo-first-order rate constants (k_r) increase markedly with increase of p[H^+]. This is expected because more unprotonated hydrazine is present, but it is not the only reason for the change in k_r values. We find strong evidence for buffer-assisted increase of the reaction rates. Figure 2 shows that the k_r values increase in direct proportion to OAc^- concentration at p[H^+] = 4.68 ± 0.03 and in direct proportion to HPO_4^{2-} concentration

(13) Jeffrey, G. H.; Bassett, J.; Mendham, J.; Denney, R. C. *Vogel's Textbook of Quantitative Chemical Analysis*, 5th ed.; Wiley: New York, 1989; p 402.
(14) Awtrey, A. D.; Connick, R. E. *J. Am. Chem. Soc.* **1951**, *73*, 1341−1348.
(15) Dickson, P. N.; Margerum, D. W. *Anal. Chem.* **1986,** *58*, 3153−3158.
(16) Jacobs, S. A.; Nemeth, M. T.; Kramer, G. W.; Ridley, T. Y.; Margerum, D. W. *Anal. Chem.* **1984**, *56*, 1058−1065.
(17) Nemeth, M. T.; Fogelman, K. D.; Ridley, T. Y.; Margerum, D. W. *Anal. Chem.* **1987**, *59*, 283−291.
(18) Fogelman, K. D.; Walker, D. M.; Margerum, D. W. *Inorg. Chem.* **1989**, *28*, 986−993.
(19) Bowers, C. P.; Fogelman, K. D.; Nagy, J. C.; Ridley, T. Y.; Wang, Y. L.; Evetts, S. W.; Margerum, D. W. *Anal. Chem.* **1997**, *69*, 431−438.
(20) McDonald, M. R.; Wang, T. X.; Gazda, M.; Scheper, W. M.; Evetts, S. W.; Margerum, D. W. *Anal. Chem.* **1997**, *69*, 3513−3520.

Table 1. Rate Constant Dependence on Hydrazine Concentration Measured in 0.91 M $HClO_4$[a,b] and at p[H^+] 7.1−7.6[a,c]

$[N_2H_4]_T$, mM	p[H^+]	k_r, s^{-1}
4.00	0.040	0.13×10^{-3}
60.0	0.040	3.02×10^{-3}
100.0	0.040	5.62×10^{-3}
10.0	7.12	1.25×10^{3}
13.0	7.16	1.93×10^{3}
15.0	7.16	2.59×10^{3}
18.0	7.22	3.47×10^{3}
20.0	7.23	4.45×10^{3}
10.0	6.95	0.81×10^{3}
10.0	7.17	1.81×10^{3}
10.0	7.40	2.83×10^{3}
10.0	7.55	4.06×10^{3}

[a] Conditions: 25.0 °C, $\lambda = 353$ nm, $[I_2]_T = 2.0 \times 10^{-4}$ M. [b] At pH = 0.040: $[N_2H_4]_T = [N_2H_4] + [N_2H_5^+] + [N_2H_6^{2+}]$, $\mu = 1.0$ M ($HClO_4$ + $NaClO_4$); $[I^-] = 0.010$ M. [c] PAF-PRO measurements: $[N_2H_4]_T = [N_2H_4] + [N_2H_5^+] + [I_2N_2H_4]$, $\mu = 0.50$ M ($NaClO_4$), $[I^-] = 0.0400$ M.

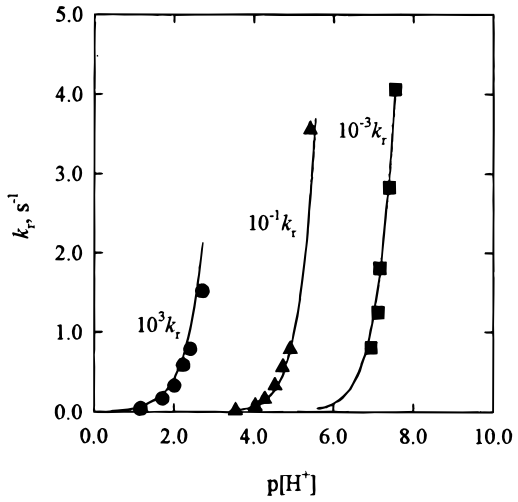

Figure 1. Effect of pH on the observed rate constant: (●) $10^3 k_r$, no buffer, $[I^-] = 0.100$ M, $[N_2H_4]_T = 2.00$ mM; (▲) $10^{-1} k_r$, $[HOAc]_T = 0.20$ M, $[I^-] = 0.020$ M, $[N_2H_4]_T = 2.03$ mM, stopped-flow measurements; (■) $10^{-3} k_r$, hydrazine self-buffer $[N_2H_4]_T = 2.00$ mM, $[I^-] = 0.100$ M, PAF-PRO measurements. The curved lines are calculated from eq 15.

at p[H^+] = 5.98 ± 0.04. Data at higher pH indicate that the rates are accelerated by the basic form of each buffer. In addition, the PAF-PRO method provides excellent kinetic evidence for formation of an iodine-hydrazine adduct, $I_2N_2H_4$. On the basis of these observations we propose the general base-assisted mechanism given in eqs 7−15 above pH 1. At 25.0 °C and $\mu = 0.50$ M, the value for K_I is 721 M^{-1}.[21] A value of 1.15×10^8 M^{-1} for K_{P1} was measured in this work by potentiometric titration with $\mu = 0.50$ M ($NaClO_4$), $T = 25$ °C; the value is in good agreement with Ware's result.[22] The rate constant for I_3^- formation in eq 7 is 5.6×10^9 M^{-1} s^{-1},[23] and the protonation rate constant in eq 8 to give $N_2H_5^+$ should be about 10^{10} M^{-1} s^{-1},[24] so the reactions in eqs 7 and 8 are in rapid equilibria.

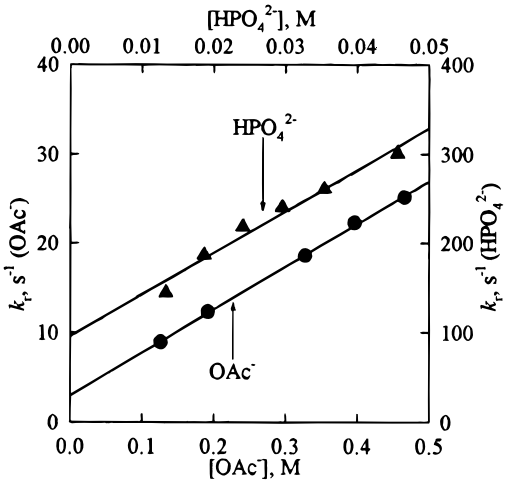

Figure 2. Evidence for general base assistance by buffer bases. (●) Bottom abscissa, acetate dependence at pH 4.7, $[I^-] = 0.0200$ M, $[N_2H_4]_T = 0.00505$ M. Slope = 48.1 M^{-1} s^{-1}, intercept = 2.95 s^{-1}. (▲) Top abscissa, phosphate dependence at pH 6.0, $[I^-] = 0.0300$ M, $[N_2H_4]_T = 0.00202$ M. Slope = 4.67×10^3 M^{-1} s^{-1}, intercept = 95.7 s^{-1}.

Proposed Mechanism above pH 1.0

$$I_2 + I^- \overset{K_1}{\rightleftharpoons} I_3^- \quad (7)$$

$$N_2H_4 + H^+ \overset{K_{P1}}{\rightleftharpoons} N_2H_5^+ \quad (8)$$

$$I_2 + N_2H_4 \overset{K_A}{\rightleftharpoons} I_2N_2H_4 \quad (9)$$

$$I_2N_2H_4 \underset{k_{-1}}{\overset{k_1}{\rightleftharpoons}} IN_2H_4^+ + I^- \quad (10)$$

$$IN_2H_4^+ \xrightarrow{k_2} I^- + N_2H_3^+ + H^+ \quad (11)$$

$$I_2N_2H_4 + B \xrightarrow{k_3^B} IN_2H_3 + HB^+ + I^- \quad (12)$$

$$IN_2H_3 \xrightarrow{\text{rapid}} I^- + N_2H_2 + H^+ \quad (13)$$

$$N_2H_3^+ \xrightarrow{\text{rapid}} N_2H_2 + H^+ \quad (14)$$

$$N_2H_2 + I_2 \xrightarrow{\text{rapid steps}} N_2 + 2H^+ + 2I^- \quad (15)$$

Primary, secondary, and tertiary amines form adducts with iodine in *n*-heptane solutions.[25,26] A crystal structure has been determined for $(CH_3)_3NI_2$.[27] Hydroxylamine and iodine form the adduct I_2NH_2OH in aqueous solution with a stability constant (K_A) of 480 M^{-1}.[28] While the nucleophilicity of hydrazine is reported to be the same as that of hydroxylamine ($\eta = 6.60$),[29] hydrazine (pK_a 8.06) is a stronger Brønsted base than hydroxylamine (pK_a 6.00). Therefore, we expect adduct formation to give $I_2N_2H_4$ in reaction 9, where the formation rate constant should be near the diffusion-limiting value of 7×10^9 M^{-1} s^{-1}.[12] Our data indicate that $I_2N_2H_4$ decays to form $IN_2H_4^+$ as a steady-state species (eq 10 and 11), in general agreement with the

(21) Ramette, R. W.; Sandford, R. W. *J. Am. Chem. Soc.* **1965**, *87*, 5001−5005.
(22) Ware, G. C.; Spulnik, J. B.; Gilbert, E. C. *J. Am. Chem. Soc.* **1936**, *58*, 1605−1606.
(23) Ruasse, M.; Aubard, J.; Galland, B.; Adenier, A. *J. Phys. Chem.* **1986**, *90*, 4382−4388.
(24) Eigen, M. *Angew. Chem., Int. Ed. Engl.* **1964**, *3*, 1−19.
(25) Drago, R. S.; Meek, D. W.; Longhi, R.; Joesten, M. D. *Inorg. Chem.* **1963**, *2*, 1056−1060.
(26) Yada, H.; Tanaka, J.; Nagakura, S. *Bull. Chem. Soc. Jpn.* **1960**, *33*, 1660−1667.
(27) Strømme, K. O. *Acta Chem. Scand.* **1959**, *13*, 268−274.
(28) Liu, R. M.; McDonald, M. R.; Margerum, D. W. *Inorg. Chem.* **1995**, *34*, 6093−6099.
(29) Pearson, R. G.; Sobel, H.; Songstad, J. *J. Am. Chem. Soc.* **1968**, *90*, 319−326.

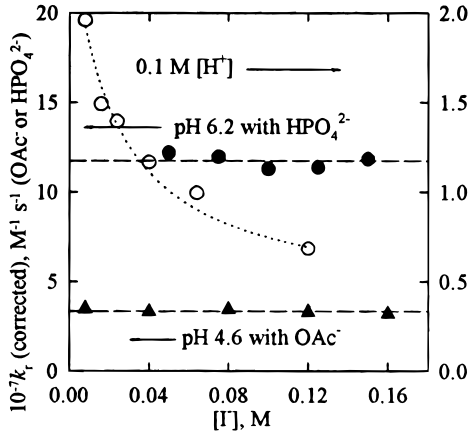

Figure 3. Iodide ion dependence of the observed rate constants (corrected for the formation of I_3^- and $N_2H_5^+$). (○) 0.1 M H^+, $[N_2H_4]_T$ = 9.13 mM, no buffer; dotted line is calculated from eq 15. The decrease of k_r(corrected) with $[I^-]$ indicates additional I^- suppression. (▲) pH 4.6, $[HOAc]_T$ = 0.20 M, $[N_2H_4]_T$ = 7.66 mM. The horizontal line indicates no additional suppression of the rate by I^-. (●) pH 6.2, $[HPO_4^{2-}]_T$ = 0.050 M, $[N_2H_4]_T$ = 2.01 mM. The horizontal line indicates no additional suppression of the rate by I^-.

mechanism of King et al.,[6] although at low pH they did not have appreciable adduct formation. In addition, our experimentally determined log K_{P1} = 8.06 (vs their value of 8.5) changes the value of the rate constant. We also find that $I_2N_2H_4$ also undergoes a general base-assisted deprotonation (eq 12) to give IN_2H_3. The rate-limiting steps in the proposed mechanism are attributed to the loss of the $IN_2H_4^+$ steady-state species (eqs 10 and 11) and to the general base-assisted reactions with $I_2N_2H_4$ (eq 12). The latter reaction becomes the dominant pathway as the pH and buffer concentrations increase. A second I_2 must react rapidly after the rate-determining steps. We propose IN_2H_3, $N_2H_3^+$, and N_2H_2 as intermediates that react in a series of rapid steps to give N_2.

If we define the rate in accord with eq 4, we can derive the expression in eq 16 for the pseudo-first-order rate constant,

$$k_r = \frac{2[N_2H_4]_T\left(\dfrac{k_1K_A}{1+(k_{-1}/k_2)[I^-]} + \sum k_3^B K_A[B]\right)}{(1+K_I[I^-]+K_A[N_2H_4])(1+K_{P1}[H^+])} \quad (16)$$

where the factor of 2 accounts for the stoichiometric ratio of two iodines with one hydrazine and the equilibrium and rate constants correspond to those in the mechanism. The proposed mechanism and the rate expression are moderately complicated, but we can treat them under different pH regions where some terms and contributions become negligible and we will show how the kinetic data support the proposed mechanism.

Iodide Ion Concentration Dependence. If the decrease in the reaction rate constants as I^- concentration increases were due solely to the formation of I_3^-, then the rate constants corrected for the formation of I_3^- should be independent of $[I^-]$. This is the case for both the HPO_4^{2-} and OAc^- data in Figure 3 which plots k_r(corrected) against $[I^-]$, where the left-hand ordinate is k_r(corrected) = k_r $(1 + K_I[I^-] + K_A[N_2H_4])(1 + K_{PI}[H^+])/2[N_2H_4]_T$. (As will be shown later, contributions from the $K_A[N_2H_4]$ term are negligible below pH 5 and almost negligible at p$[H^+]$ 6.2.) Within experimental error, the horizontal lines in Figure 3 for both the HPO_4^{2-} and the OAc^- data indicate the absence of additional I^- suppression of the reaction under these conditions. On the other hand, Figure 3 also shows data in 0.1 M $[H^+]$, where the right-hand ordinate is k(corrected) = $k_r(1 + K_I[I^-])(1 + K_{P1}[H^+] + K_{P1}K_{P2}[H^+]^2)/2[N_2H_4]_T$. (At this acidity a small amount of $N_2H_6^{2+}$ is present and the correction takes this into account.) The decrease in k_r(corrected) values as the I^- concentration increases clearly shows an additional source of I^- suppression which is in agreement with the observations of King et al.[6] This can be accounted for by eq 10 in the mechanism, where the reverse reaction of I^- with the steady-state intermediate, $IN_2H_4^+$, inhibits the rate. The $k_1K_A/[1 + (k_{-1}[I^-]/k_2)]$ term in the numerator of eq 16 can be used to fit the data.

The overall mechanism must explain why the additional $[I^-]$ suppression disappears in the acetate and phosphate buffer reactions. Equation 11 proposes the loss of I^- and the transfer of a proton from $IN_2H_4^+$ to the solvent, but OAc^- and HPO_4^{2-} would be expected to assist greatly in proton abstraction as shown in eq 17. If this were the case, a consequence would be

$$IN_2H_4^+ + B \xrightarrow{k_2^B} I^- + N_2H_3^+ + HB^+ \quad (17)$$

that $k_2^B[B] \gg k_{-1}[I^-]$, so that $k_{-1}[I^-]/(k_2 + k_2^B[B]) \ll 1$. As a result the first numerator term in eq 16 becomes simply $2[N_2H_4]_TK_Ak_1$. Thus, the additional I^- suppression disappears and the $k_2^B[B]$ term also drops out. If this were the only source of base assistance, the buffer effects shown in Figure 2 would not occur. Hence, the direct reaction of bases with $I_2N_2H_4$ in eq 12 of the mechanism is necessary to explain the buffer effects. The strong base assistance in eq 12 makes it impossible to determine k_2^B values in eq 17. The horizontal line for the OAc^- data in Figure 3 indicates that under these conditions $(k_2 + k_2^{OAc}[OAc^-]) \gg k_{-1}[I^-]$. A similar inequality would be expected for the HPO_4^{2-} reactions.

Kinetics with Acetate Buffer. We disagree with one of the recent studies[11] that claimed no general base-assisted effect from their acetate dependence study. Figure 2 clearly shows that buffer base accelerates the reaction rates. At pH 4.63 with acetate buffer present, the rate expression eq 16 can be simplified to give eq 18 because the $K_A[N_2H_4]$ term is much less than

$$k_r = 2[N_2H_4]_T\frac{(k_1K_A + k_3^{H_2O}K_A + k_3^{OAc}K_A[OAc^-])}{(1+K_I[I^-])(1+K_{P1}[H^+])} \quad (18)$$

unity and the $[I^-]$ term in the numerator drops out due to the reaction in eq 17. Thus, the rate-determining steps become k_1 and k_3^B. From the intercept and slope of Figure 2, we can resolve values for H_2O and OAc^- as bases to give the rate constants: $(k_1K_A + k_3^{H_2O}K_A) = 1.8 \times 10^7$ M^{-1} s^{-1} and $k_3^{OAc}K_A = 1.5 \times 10^8$ M^{-1} s^{-1}.

The p$[H^+]$ dependence study with buffer $[HOAc]_T$ = 0.20 M in Figure 1 shows excellent agreement between the experimental data (solid triangles) and the predicted values (solid line) based on eq 18. This supports the validity of these values ($k_1K_A + k_3^{H_2O}K_A$ and $k_3^{OAc}K_A$) as well as the proposed mechanism.

Hydrazine as a Nucleophile as Well as a General Base. In the proposed mechanism, hydrazine acts as a nucleophile to form an iodine adduct ($I_2N_2H_4$) which undergoes general base reactions. Since hydrazine is also a Brønsted base with a pK_a of 8.06 for $N_2H_5^+$, in high $[N_2H_4]$ we would expect hydrazine to react with $I_2N_2H_4$ as a general base in eq 12 in addition to acting as a nucleophile in eq 9. Substitution of $[N_2H_4]$ for [B] in eq 16 gives a numerator that contains both $[N_2H_4]$ and $[N_2H_4]^2$ terms. The PAF-IO (model IV) was used to study the k_r dependence of N_2H_4 and OH^- with excess hydrazine present as a buffer at pH ~ 7.5. Under these conditions, the formation

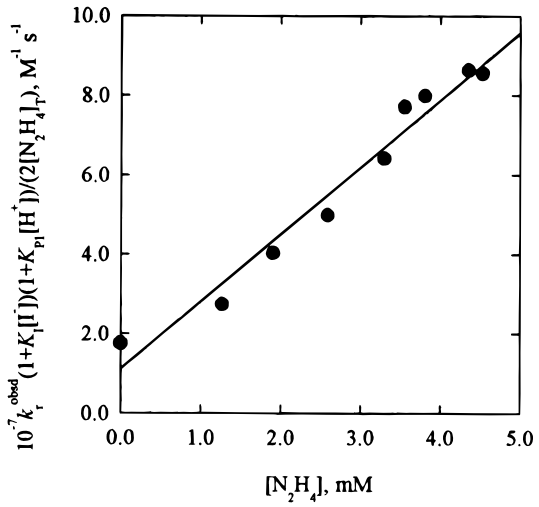

Figure 4. Observed rate constants (corrected for the formation of I_3^- and $N_2H_5^+$) as a function of excess $[N_2H_4]$ at p$[H^+]$ 7.2, $[I^-] = 0.0400$ M measured on the PAF-IO. The positive slope indicates that hydrazine acts as a general base as well as a nucleophile since the ordinate values are already corrected for hydrazine as a nucleophile. Intercept $= 1.1 \times 10^7$ M^{-1} s^{-1}, slope $= k_3^{N_2H_4}K_A = 1.7 \times 10^{10}$ M^{-2} s^{-1}.

of $I_2N_2H_4$ is appreciable compared with I_3^- formation, which results in the decrease of A_o that is calculated for the postmixed I_3^-/I_2 solution before it reacts with N_2H_4. Consequently, the measured pseudo-first-order rate constants (k_r^{obsd}) are too large since k_r^{obsd} measured by the PAF-IO depends on A_o (eq 5). Nonetheless, we can correct the measured rate constant k_r^{obsd} to the true rate constant k_r based on the ratio of $I_3^-/(I_2 + I_3^- + I_2N_2H_4)$ as shown in eq 19, where $K_A = [I_2N_2H_4]/[I_2][N_2H_4]$. The k_r^{obsd} values (although they are not true rate constants due to the decrease of A_o) can be used to evaluate the rate constants of $k_3^{N_2H_4}$ and k_3^{OH} and to seek evidence that hydrazine acts both as a nucleophile and as a general base. Combining eq 19 with eq 16 gives the rate expression as eq 20, where k_r^{obsd} is the

$$k_r = \frac{k_r^{obsd}(1 + K_I[I^-])}{1 + K_I[I^-] + K_A[N_2H_4]} \tag{19}$$

measured pseudo-first-order rate constant. Figure 4 shows a

$$\frac{k_r^{obsd}(1 + K_{P1}[H^+])(1 + K_I[I^-])}{2[N_2H_4]_T} = k_1K_A + k_3^{H_2O}K_A + k_3^{OH}K_A[OH^-] + k_3^{N_2H_4}K_A[N_2H_4] \tag{20}$$

plot of the left-hand side of eq 20 against $[N_2H_4]$ with the slope value of 1.7×10^{10} M^{-2} s^{-1} that corresponds to $k_3^{N_2H_4}K_A$. This shows that hydrazine acts as a general base as well as a nucleophile, otherwise we would obtain a horizontal line in Figure 4 because the ordinate values are already corrected for the hydrazine term as a reductant. In accord with eq 20, we also evaluate the rate constant $k_3^{OH}K_A = 9.5 \times 10^{12}$ M^{-2} s^{-1} by variation of $[OH^-]$ from p$[H^+]$ 6.93 to 7.98 at constant $[N_2H_4]_T = 0.0100$ M.

Kinetic Evaluation of the Equilibium Constant for $I_2N_2H_4$ Formation. The PAF-IO data permit us to evaluate the rate constants of $k_3^{N_2H_4}K_A$ and $k_3^{OH}K_A$. In order to obtain an evidence for the formation of an adduct $I_2N_2H_4$ and the equilibrium constant value of K_A, we need to measure the true rate constant k_r values under similar conditions to those used with the PAF-IO experiments where the formation of $I_2N_2H_4$ is sufficient to change the initial absorbance due to conversion of I_3^- to $I_2N_2H_4$. The pulsed−accelerated-flow spectrometer with position-resolved observation (PAF-PRO) provides this capability. With the PAF-PRO instrument an appreciable degree of mixing occurs before the observation but measurements perpendicular to the flow direction permit the true extent of the reaction to be determined. Extremely fast reactions to form $I_2N_2H_4$ decreases the initial absorbance due to I_3^- loss and this decrease of A_o is larger as the N_2H_4 concentration increases. The rate constants measured on this instrument are true k_r values since they are independent of A_0 (eq 5). Under similar conditions as the above PAF-IO experiment, the pseudo-first-order rate constants were collected on the PAF-PRO and are given in Table 1. These data were fit using eq 21 along with the previously resolved rate constants. The nonlinear fit results

$$k_r = \frac{2[N_2H_4]_TK_A(k_1 + k_3^{H_2O} + k_3^{OH}[OH^-] + k_3^{N_2H_4}[N_2H_4])}{(1 + K_I[I^-] + K_A[N_2H_4])(1 + K_{P1}[H^+])} \tag{21}$$

in a K_A value of $(2.0 \pm 0.1) \times 10^4$ M^{-1}. This value for the association constant is much greater than the corresponding I_2-NH_2OH adduct (480 M^{-1})[28] and is much smaller than the $I_2S_2O_3^{2-}$ adduct (3.2×10^7 M^{-1}).[30]

Phosphate Buffer Dependence. Janovsky reported[10] that the reaction rate is catalyzed by phosphate buffer due to the formation of a $N_2H_4{\cdot}HPO_4^{2-}$ complex. Since both N_2H_4 and HPO_4^{2-} are bases, they are unlikely to form a complex. Instead we suggest that HPO_4^{2-} acts as a general base (as is the case for OAc^-, N_2H_4, and OH^-) to accelerate the reaction rate. To test this effect, a phosphate dependence study at p$[H^+]$ 6.4 was performed on the Durrum stopped-flow. Under these conditions, the formation of $I_2N_2H_4$ must be considered and the rate expression of eq 16 includes the rate constants of k_3^{OH}, $k_3^{N_2H_4}$, and $k_3^{HPO_4}$, while the k_{-1} $[I^-]/k_2$ term drops out. The slope of the phosphate dependence in Figure 2 gives a $k_3^{HPO_4}K_A$ value of 4.0×10^9 M^{-2} s^{-1} in accord with eq 16.

Brønsted−Pedersen Relationship. A plot of the Brønsted−Pedersen relationship[31] (eq 22)

$$\log(k_3^B/q) = \log G_B + \beta \log(p/K_aq) \tag{22}$$

for the k_3^B terms is given in Figure 5, where the pK_a^{HB} values are −1.73 (H_3O^+), 4.41 (HOAc),[32] 6.46 ($H_2PO_4^-$),[33] 8.06 ($N_2H_5^+$), and 15.34 (H_2O);[34] p is the number of equivalent protons on HB, and q is the number of equivalent basic sites on B. In this plot, the $k_3^{H_2O}$ value of 1.8×10^2 s^{-1} for water is divided by 55.5 M to give a second-order rate constant of 3.2 M^{-1} s^{-1} that is comparable to the second-order rate constants for the other bases. The log G_B value is 1.4, and the slope (β) is 0.46, which indicates a transition state with a significant degree of proton transfer from $I_2N_2H_4$ to B. We propose that I^- leaves as the proton is transferred to give a transition state of $[I^{(-)}\text{- - -}IN_2H_3\text{- - -}H^{(+)}\text{- - -B}]$ which leads to the formation of IN_2H_3 as a reactive intermediate species. The general-base assistance requires that proton transfer take place in the rate-

(30) Scheper, W. M.; Margerum, D. W. *Inorg. Chem.* **1992**, *31*, 5466−5473.
(31) Bell, R. P. *The Proton in Chemistry*, 2nd ed.; Cornell University Press: Ithaca, NY, 1973; p 198.
(32) Urbansky, E. T.; Cooper, B. T.; Margerum, D. W. *Inorg. Chem.* **1997,** *36*, 1338−1344.
(33) Mesmer, R. E.; Baes, C. F. *J. Solution Chem.* **1974**, *3*, 307−321.
(34) Molina, M.; Melios, C.; Tognolli, J. O.; Luchiari, M., Jr. *J. Electroanal. Chem. Interfacial Electrochem.* **1979**, *105*, 237−246.

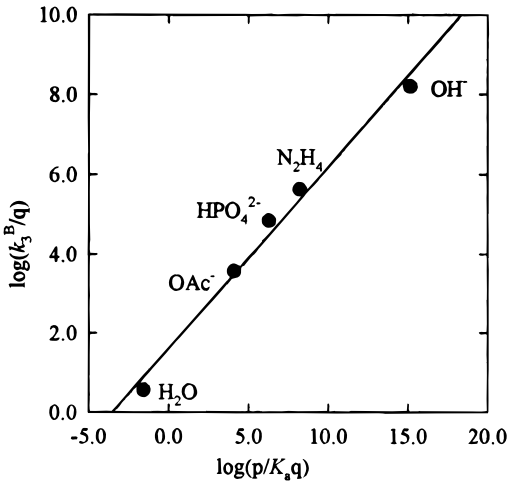

Figure 5. Brønsted−Pedersen plot of the rate constants for the general base-assisted proton-transfer reactions with $I_2N_2H_4$. The slope (β) is 0.46.

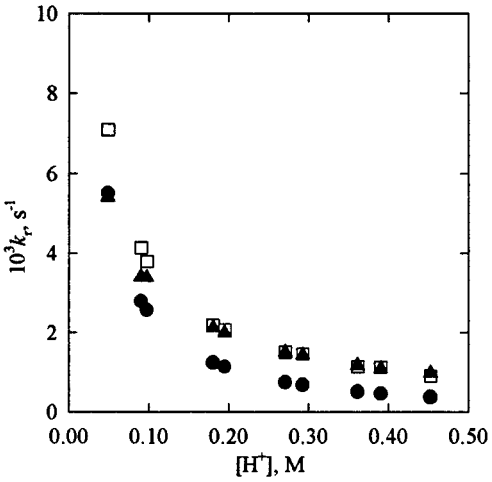

Figure 6. Dependence of the observed rate constant on $[H^+]$. (▲) Experimental data. (□) Fitted values based on eq 25 that considers $N_2H_5^+$ as a reactive species. The agreement between the experimental data and fitted values support the $N_2H_5^+$ pathway. The nonlinear fit yields $k_1K_A = 1.4 \times 10^7$ M^{-1} s^{-1} for the N_2H_4 pathway, $k'_1K'_A = 0.7$ M^{-1} s^{-1} for the $N_2H_5^+$ pathway, $k_3^{H_2O}K_A = 4.0 \times 10^6$ M^{-1} s^{-1} for H_2O as a base pathway, $k_{-1}/k_2 = 20$ M^{-1}, and $k'_{-1}/k_2 = 100$ M^{-1}. (●) Calculated values based on eq 15, which assumes $N_2H_5^+$ is unreactive.

determining step. An alternative two-step path could first generate $I_2N_2H_3^-$ as a very reactive species that rapidly loses I^-.

Proposed Mechanism in High Acid Concentrations. As the H^+ concentration is increased above 0.1 M, appreciable concentrations of the doubly protonated hydrazine species, $N_2H_6^{2+}$, form. A value of 1.61 M^{-1} for K_{P2} (eq 23) has been

$$N_2H_5^+ + H^+ \overset{K_{P2}}{\rightleftharpoons} N_2H_6^{2+} \qquad (23)$$

determined at 25.0 °C and $\mu = 0.50$ M.[35] Other kinetic studies in this laboratory[36] have shown that Br_2 reacts with $N_2H_5^+$ but does not react with $N_2H_6^{2+}$. We tested I_2 reactions with increasing acidity up to 0.45 M $[H^+]$ and found evidence for reactions between I_2 and $N_2H_5^+$ but not between I_2 and $N_2H_6^{2+}$. Equations 24 and 25

$$I_2 + N_2H_4 \overset{K_A}{\rightleftharpoons} I_2N_2H_4 \overset{k_1}{\underset{k_{-1}}{\rightleftharpoons}} I^- + IN_2H_4^+ \qquad (24)$$

$$I_2 + N_2H_5^+ \overset{K'_A}{\rightleftharpoons} I_2N_2H_5^+ \overset{k'_1}{\underset{k'_{-1}}{\rightleftharpoons}} I^- + IN_2H_4^+ + H^+ \qquad (25)$$

give the proposed parallel paths for the reactions of I_2 with N_2H_4 and with $N_2H_5^+$, respectively. In acid solutions the concentrations of both $I_2N_2H_4$ and $I_2N_2H_5^+$ are negligible. The rate expression in eq 16 is modified to give eq 26,

$$k_r = \frac{2[N_2H_4]_T\left(\dfrac{k_1K_A + k'_1K'_AK_{P1}[H^+]}{1 + (k_{-1}/k_2)[I^-] + (k'_{-1}/k_2)[I^-][H^+]} + k_3^{H_2O}K_A\right)}{(1 + K_I[I^-])K_{P1}[H^+](1 + K_{P2}[H^+])} \qquad (26)$$

where $[N_2H_4]_T = [N_2H_4] + [N_2H_5^+] + [N_2H_6^{2+}]$. The reactions are very slow in high acid because the $I_2/N_2H_5^+$ pathway is seven orders of magnitude slower than the I_2/N_2H_4 pathway. Figure 6 plots the k_r values against $[H^+]$. The solid circles show the expected behavior if $N_2H_5^+$ was not reactive. The actual behavior from the experimental results is given by the solid triangles. By using the previously determined value of ($k_1K_A + k_3^{H_2O}K_A$) = 1.8×10^7 M^{-1} s^{-1} from the acetate dependence data and the microscopic reversibility relationship ($k_1K_A/k_{-1} = k_1'K_A'K_{P1}/k_{-1}'$), we can fit the data at high $[H^+]$ to eq 26. A nonlinear fit of these data gives values of $k_1K_A = 1.4 \times 10^7$ M^{-1} s^{-1}, $k_1'K_A' = 0.7$ M^{-1} s^{-1}, $k_3^{H_2O}K_A = 4.0 \times 10^6$ M^{-1} s^{-1}, $k_{-1}/k_2 = 20$ M^{-1}, and $k_{-1}'/k_2 = 1.0 \times 10^2$ M^{-2}. The fitted values (open squares in Figure 6) agree with the experimental data. Table 2 gives the equilibrium and rate constants evaluated for the full mechanism. Our value for K_Ak_1 is 1.4×10^7 M^{-1} s^{-1}; the corresponding value by King et al.[6] (eq 2) becomes 1.6×10^7 M^{-1} s^{-1} when a log K_{P1} value of 8.06 is used rather than their value of 8.5. So these values are in agreement within experimental error. Our k_{-1}/k_2 value of 20 M^{-1} is larger than their value of 12 M^{-1} because they were not aware of contributions from the reaction path in eq 25.

Table 2. Summary of Equilibrium and Rate Constants[a]

constant	value
K_I	721 M^{-1} [b]
K_{P1}	1.15×10^8 M^{-1} [c,d]
K_{P2}	1.61 M^{-1} [e]
K_A	$(2.0 \pm 0.1) \times 10^4$ M^{-1}
k_1	$(7.0 \pm 0.3) \times 10^2$ s^{-1}
$k_1'K_A'$	0.7 ± 0.2 M^{-1} s^{-1}
k_{-1}/k_2	20 ± 5 M^{-1}
k_{-1}'/k_2	$(1.0 \pm 0.1) \times 10^2$ M^{-2}
k_3^{OAc}	$(7.5 \pm 0.2) \times 10^3$ M^{-1} s^{-1}
$k_3^{HPO_4}$	$(2.0 \pm 0.4) \times 10^5$ M^{-1} s^{-1}
$k_3^{N_2H_4}$	$(8.5 \pm 0.3) \times 10^5$ M^{-1} s^{-1}
k_3^{OH}	$(4.8 \pm 1.0) \times 10^8$ M^{-1} s^{-1}
$k_3^{H_2O}$	$(2.0 \pm 0.5) \times 10^2$ s^{-1}
$k_3^{H_2O}$/55.5 (Figure 5)	3.6 M^{-1} s^{-1}

[a] Conditions: 25.0 °C, $\mu = 0.50$ M. [b] Reference 21. [c] This work. [d] Reference 22. [e] Reference 35.

Electron-Transfer vs Ion-Transfer Mechanisms. As an alternate mechanism, could the redox reaction between iodine and hydrazine take place by an electron-transfer process such as eq 27? Self-exchange rate constants for I_2/I_2^- ($k_{11} = 8.5 \times$

(35) Jia, Z.; Margerum, D. W. To be submitted for publication.
(36) Salaita, M.; Liu, R. M.; Margerum, D. W. Unpublished results.

$$I_2 + N_2H_4 \overset{k_{12}}{\rightleftharpoons} I_2^{\bullet -} + N_2H_4^{\bullet +} \quad (27)$$

10^4 M^{-1} s^{-1})[37] and for $N_2H_4^+/N_2H_4$ ($k_{22} \leq 0.3$ M^{-1} s^{-1})[38] can be used with the $E°$ values[39] and Marcus theory[40] to estimate a value for a $k_{12} \leq 4.8 \times 10^{-3}$ M^{-1} s^{-1} in eq 27. This is about 9 orders of magnitude smaller than the measured rate constants ($K_A k_3^{H_2O} = 4.0 \times 10^6$ M^{-1} s^{-1} and $K_A k_1 = 1.4 \times 10^7$ M^{-1} s^{-1}) without general base assistance. Hence, this electron-transfer path can be ruled out.

In our proposed mechanism, the redox process is initiated by a very rapid reaction between electrophilic iodine and nucleophilic hydrazine (eq 9) to form the adduct, $I_2N_2H_4$. Similar reactions between iodine and thiosulfate ion[30] and between iodine and iodide ion[23] occur with diffusion-controlled rate constants. At low pH the $I_2N_2H_4$ adduct reacts by loss of I^- (eq 10) to form $IN_2H_4^+$, a steady-state intermediate that decomposes to give $N_2H_3^+$ (eq 11). Evidence for a free radical $N_2H_4^{\bullet +}$ has been provided by ESR spectroscopy;[41] $N_2H_3^\bullet$ has been generated by pulse radiolysis and detected by UV spectroscopy.[42] The proposed $IN_2H_4^+$ and IN_2H_3 intermediate species in our mechanism should be energetically more favorable than these free radical species. In the presence of general bases (OAc^-, HPO_4^{2-}, N_2H_4, OH^-), the mechanism shifts to eq 12, where proton abstraction from $I_2N_2H_4$ becomes the rate-determining step accompanied (or immediately followed) by I^- loss to give IN_2H_3. Subsequent reaction steps are rapid (eqs 13−15) and consume another I_2 to produce N_2. It is possible that IN_2H_3 reacts directly with I_2 or that N_2H_2 (diazine) forms first and then reacts with I_2. In either case the reactions are too rapid to be observed.

Comparison with Hydroxylamine. The mechanism of iodine oxidation of hydrazine has many similarities with its oxidation of hydroxylamine.[28] For hydroxylamine the first step is the formation of an adduct, I_2NH_2OH, with a stability constant of 480 M^{-1}. This adduct undergoes general base-assisted deprotonation to give INHOH, a steady-state intermediate that decays to form HNO. Subsequent rapid dehydrative dimerization of HNO gives N_2O as the final product. The stability constant of 2×10^4 M^{-1} for the hydrazine adduct ($I_2N_2H_4$) is a factor of 42 larger than for the hydroxylamine adduct I_2NH_2OH. Since the general base-assisted rate constants are factors of 4−40 larger for reactions with I_2NH_2OH than with $I_2N_2H_4$, the ratio of $K_A k^B$ values for hydroxylamine compared to hydrazine vary from 0.1 to 1.0. The pK_a values are 8.06 for hydrazine and 6.00 for hydroxylamine, so below pH 6 the observed rates for iodine with hydroxylamine are faster than with hydrazine.

Scheme 1. General Base-Assisted Pathways for I_2 Reactions with Hydrazine and Hydroxylamine

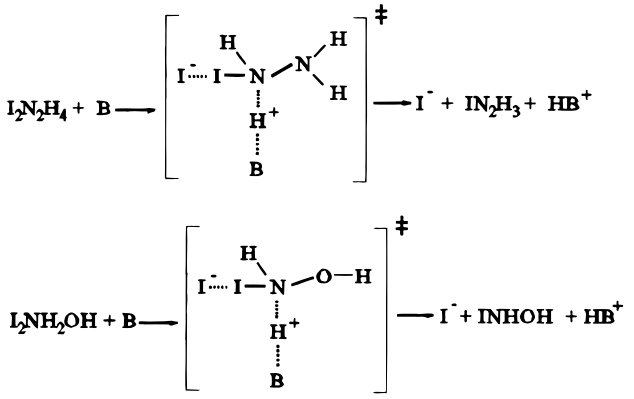

Scheme 1 shows the proposed transition states for the general base-assisted deprotonation of the iodine adducts of hydrazine and hydroxylamine, where I^- loss accompanies the proton transfer. The Brønsted β value is 0.46 for the reaction of $I_2N_2H_4$, while it is 0.58 for the reaction of I_2NH_2OH. Although there appears to be a higher degree of proton transfer in the transition state of the hydroxylamine adduct, the base-assisted pathways are very similar.

Conclusions. The oxidation of hydrazine by iodine proceeds by adduct formation followed by general base-assisted loss of H^+ accompanied by I^- loss. The overall oxidation process to give N_2 is equivalent to an I^+ transfer and subsequent I^- elimination. Similar halogen−cation transfer steps and halide ion elimination steps are observed for the reactions of many active halogen oxidants with nitrogen nucleophiles.[43−46]

Acknowledgment. This investigation was supported by National Science Foundation Grants CHE-9024291 and CHE-9622683.

Supporting Information Available: Listings of kinetic data (5 pages). Ordering information is given on any current masthead page.

IC970753V

(37) Woodruff, W. H.; Margerum, D. W. *Inorg. Chem.* **1974**, *13*, 2578−2585.
(38) Stanbury, D. M. *Inorg. Chem.* **1984,** *23*, 2879−2882.
(39) Stanbury, D. M. *Adv. Inorg. Chem.* **1989**, *33*, 69−133.
(40) Marcus, R. A. *J. Chem. Phys.* **1965**, *43*, 679−701.
(41) Adams, J. Q.; Thomas, J. R. *J. Chem. Phys.* **1963,** *39*, 1904−1906.
(42) Hayon, E.; Simic, M. *J. Am. Chem. Soc.* **1972,** *94*, 42−47.
(43) Cooper, J. N.; Margerum, D. W. *Inorg. Chem.* **1993**, *32*, 5905−5910.
(44) Beckwith, R. C.; Cooper, J. N.; Margerum, D. W. *Inorg. Chem.* **1994**, *33*, 5144−5150.
(45) Johnson, D. W.; Margerum, D. W. *Inorg. Chem.* **1991**, *30*, 4845−4851.
(46) Margerum, D. W.; Schurter, L. M.; Hobson, J.; Moore, E. E. *Environ. Sci. Technol.* **1994**, *28*, 331−337.